Characterization of Terahertz Single-Photon-Sensitive Bolometric Detectors Using a Pulsed Microwave Technique

D. F. Santavicca,[*] B. Reulet,[†] B. S. Karasik,[¶] S. V. Pereverzev,[¶] D. Olaya,[‡] M. E. Gershenson,[‡] L. Frunzio,[*] and D. E. Prober[*]

[*]*Departments of Applied Physics and Physics, Yale University, New Haven, CT 06520-8284*
[†]*Laboratoire de Physique des Solides, Universite Paris-Sud, 91405 Orsay, France*
[¶]*Jet Propulsion Laboratory, California Institute of Technology, Pasadena, CA 91109*
[‡]*Department of Physics, Rutgers University, Piscataway, NJ 08854*

Abstract. We describe a technique for characterizing bolometric detectors that have sufficient sensitivity to count single terahertz photons. The device is isolated from infrared blackbody radiation and a single terahertz photon is simulated by a fast microwave pulse, where the absorbed energy of the pulse is equal to the photon energy. We have employed this technique to characterize bolometric detectors consisting of a superconducting titanium nanobridge with niobium contacts. Present devices have T_c = 0.3 K and a measured intrinsic energy resolution of approximately 6 terahertz full-width at half-maximum, near the predicted value due to intrinsic thermal fluctuation noise, with a time constant of 2 μs. An intrinsic energy resolution of 1 terahertz should be achievable by reducing the volume of the titanium nanobridge. Such a detector has important applications in future space-based terahertz astronomy missions.

Keywords: terahertz, single-photon detector, calorimeter, superconducting bolometer, energy resolution
PACS: 07.57.Kp, 85.25.Pb

INTRODUCTION

Terahertz (THz) detectors have been an active area of research during the past decade. However, an energy-resolving THz single-photon detector – i.e., a THz calorimeter – has remained elusive. Such a detector is important for proposed next-generation space-based far-infrared telescopes, which aim to achieve a sensitivity that is limited by the astronomical background photon flux [1,2]. Moderate resolution THz spectroscopy ($\lambda/\delta\lambda \sim 1000$) using an external frequency-selective element (e.g. a grating) is needed for studying star and galaxy formation. Because of the relatively low background photon arrival rate in space, photon counting becomes viable at THz frequencies [3]. Low resolution spectroscopy ($\lambda/\delta\lambda \sim$ 10-100) in the mid-infrared and THz can be performed without an external spectral dispersion element using the detector energy resolution. Applications of such a spectrometer-on-chip include studies of interstellar dust composition and the search for Earth-like exoplanets [4].

We describe a new experimental technique and its use to characterize superconducting bolometric detectors that have the sensitivity to achieve energy-resolved THz single-photon detection. These results were recently reported in [5]. This paper briefly reviews that work and provides an expanded discussion of the measurement technique.

TITANIUM BOLOMETRIC DETECTOR

The intrinsic energy resolution of a hot electron bolometric calorimeter is limited by thermodynamic fluctuations, and in simple cases scales as

$$\delta E_{intrinsic} \sim \sqrt{k_B T^2 C_e} \qquad (1)$$

where C_e is the electronic heat capacity, proportional to the active device volume and the operating temperature T [6,7]. Thus, for sensitive detection, operation is at low temperature and the active device volume is very small. Efficient coupling is achieved by integrating the device in a planar THz antenna.

The detector we have studied consists of a superconducting titanium (Ti) nanobridge approximately 4 μm long, 350 nm wide, and 70 nm thick, with T_c = 0.3 K (Fig. 1). The Ti nanobridge spans contacts consisting of thick niobium (Nb) with T_c = 8 K. The fabrication process has been described previously [8]. The dimensions of the Ti nanobridge

CP1185, *Low Temperature Detectors LTD 13, Proceedings of the 13th International Workshop*
edited by B. Cabrera, A. Miller, and B. Young

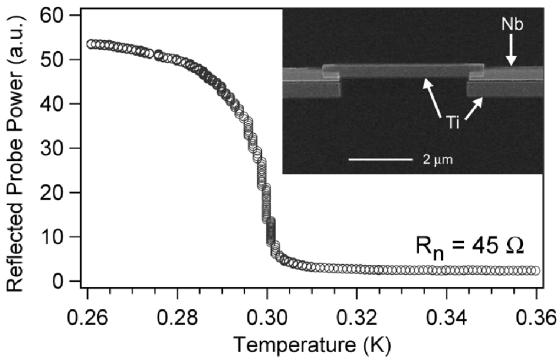

FIGURE 1. Measured reflection of the 1.3 GHz probe power as a function of temperature with $I_{dc} = 0$. Inset: SEM image of nanobolometer device on silicon substrate.

were chosen to have an impedance close to 50 Ω in the non-superconducting state to facilitate efficient high-frequency coupling.

For photons with a frequency greater than the upper frequency scale for superconductivity in the Ti, $f_{Ti} = 1.76k_BT_c/h = 11$ GHz, the nanobridge impedance is approximately equal to the normal state resistance, $R_n = 45$ Ω. In practice, the superconducting energy gap in the Ti is suppressed by the bias current, so the relevant frequency scale is below 11 GHz. The much larger superconducting energy gap in the Nb contacts prevents the outdiffusion of heat from the Ti nanobridge, and energy relaxation is set by electron-phonon coupling within the Ti, with a thermal time constant of order μs [8].

CHARACTERIZATION TECHNIQUE

A test system to study the detector response to single THz photons presents a number of technical challenges. To facilitate device characterization, we have developed an alternative testing technique that is easier to implement (Fig. 2). This technique avoids the problem of unwanted background photons and allows for a precise determination of the coupling efficiency as well as trivial adjustment of the input energy.

The device is mounted in the light-tight inner vacuum can of a ^{3}He cryostat with a base temperature of 240 mK. A single THz photon is simulated by a 20 GHz microwave pulse with a duration of 200 ns, which is much shorter than the detector time constant. The absorbed energy of the 20 GHz pulse, E_{abs}, is equal to the energy of a single higher frequency photon. We call this pulse a faux photon, or fauxton. The fauxton frequency, $f_{fauxton} = E_{abs}/h$, is adjusted simply by changing the amplitude of the microwave signal. Since 20 GHz is greater than f_{Ti}, the Ti device appears resistive at 20 GHz, with the device

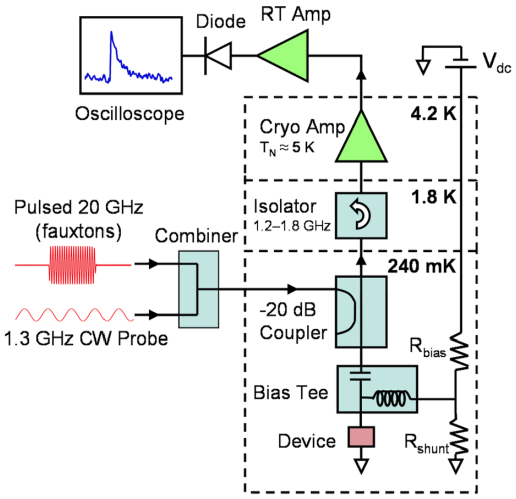

FIGURE 2. Schematic of experimental setup for fauxton testing. Solid lines represent coaxial cables, and attenuators and filters have been omitted for clarity.

impedance approximately equal to R_n, as it does for an actual THz photon.

The impedance change when a fauxton is detected is recorded by measuring the change in the reflection of a 1.3 GHz CW probe signal. The probe signal reflected by the device is amplified using a low noise cryogenic amplifier ($T_N \approx 5$ K) at 4.2 K with a cold 1.2-1.8 GHz isolator at the amplifier input. The probe signal is amplified further and band-pass filtered at room temperature, and then measured on a fast diode coupled to an oscilloscope through a low-pass filter. The bandwidth of the low-pass filter is chosen to maximize the signal-to-noise. We note that this microwave reflection readout technique is suitable for frequency-division multiplexing of a large-format detector array.

The 20 GHz coupling efficiency is calibrated in-situ using Johnson noise thermometry. With the device above T_c, we apply on the dc line a square wave audio frequency signal that switches between zero and finite voltage, and we measure the corresponding change in noise on the diode (with no probe signal). Then we apply a square-wave-modulated (on-off) 20 GHz signal, adjusting the amplitude to achieve the same noise signal on the diode. We know the power dissipated in the device by the signal from the dc line, and we use this to directly determine the coupled power at 20 GHz.

The biasing condition is set by resistors mounted at the base temperature (R_{bias} and R_{shunt} in Fig. 2). The biasing line connects to the device through the dc port of a bias-tee, which has a bandwidth from dc to 5 MHz. We used $R_{shunt} = 50$ Ω and 3 Ω. R_{shunt} determines both the dc biasing condition as well as the load line seen at all frequencies relevant to the thermal

response (R_{shunt} << R_{bias} = 1 MΩ). The optimum dc bias point is on the non-superconducting branch of the current-voltage curve, close to where the device switches back to the superconducting state, as is typical for superconducting bolometers [9].

R_{shunt} = 50 Ω corresponds approximately to the case of matched device and load impedances, in which case the effect of electrothermal feedback goes to zero [10]. In this case we should measure the intrinsic time constant $\tau_0 = C_e/G_{th}$, where G_{th} is the electron-phonon thermal conductance. We find τ_0 = 7 μs, in good agreement with [8] for T = 0.30 K. For R_{shunt} = 3 Ω, the load impedance is much less than the device impedance, and we have strong negative electrothermal feedback [10]. In this regime, the time constant becomes

$$\tau_{eff} = \tau_0 \Big/ \left[1 + (\alpha/n)\left(1 - T_s^n / T^n\right)\right] \qquad (2)$$

where α = (T/R)(dR/dT), T_s = 0.24 K is the substrate (bath) temperature, T is the device temperature (≈T_c), and n is given by $G_{th} = T^{n-1}$ [6]. We use n = 5 based on [8], and we find good agreement between the measured value of τ_{eff} = 2 μs and the calculated value using Equation (2) for α = 20.

ENERGY RESOLUTION

At different fauxton frequencies, we measure a sequence of 10^3 pulses and record each single-shot waveform. R_{shunt} = 3 Ω is used to achieve a dc voltage bias. In the linear response regime, the average peak height is proportional to the fauxton frequency. As an example, we plot in Fig. 3 a single-shot measurement of the device response to a 24 THz fauxton, as well as the average of 10^3 measurements for the same fauxton frequency. We determine the peak height at a fixed time after the trigger for each single-shot pulse using an average over a 1 μs window. For each fauxton frequency, we make a histogram of the heights of all 10^3 single-shot measurements. The histograms are fit to a Gaussian to extract the average peak height and the full-width at half-maximum (FWHM).

In Fig. 4(a), we plot the average height determined from the Gaussian fit for each fauxton frequency, with the error bars indicating the FWHM. The average peak height is linear with fauxton frequency up to approximately 24 THz. The measured response becomes sub-linear at higher fauxton frequencies, where the device begins to saturate. The saturation energy depends on multiple parameters, including the bias current, the bath temperature, and the 1.3 GHz probe power. In general, one wants to optimize these parameters to achieve the maximum response while still maintaining sufficient dynamic range for a particular experiment. The slope in the linear region

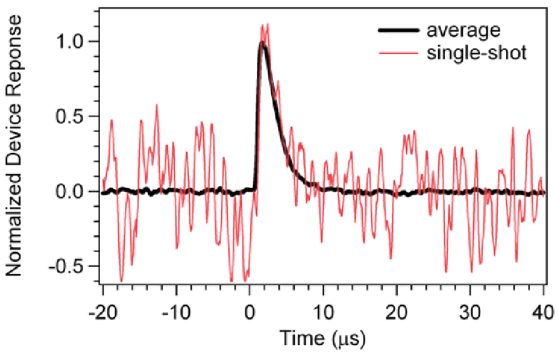

FIGURE 3. Single-shot measurement of device response to 24 THz fauxton, along with an average of 10^3 single-shot measurements for the same fauxton frequency.

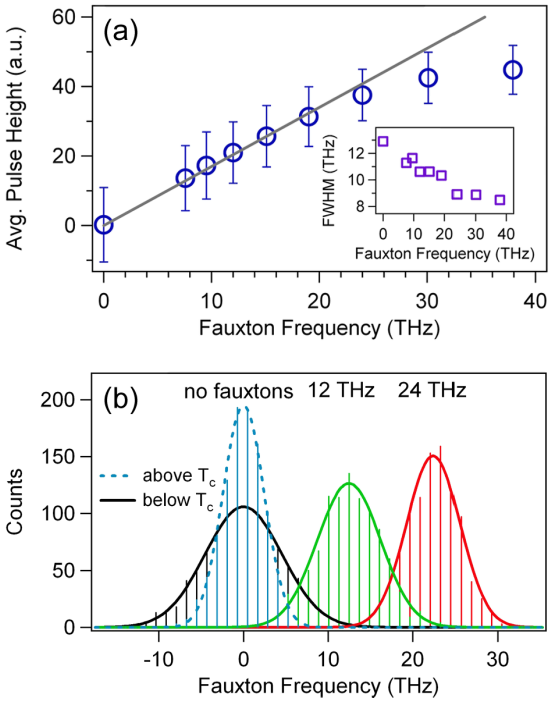

FIGURE 4. (a) Average pulse height determined from Gaussian fits as a function of fauxton frequency. Error bars indicate FWHM. Fit to linear regime (solid line) defines conversion from pulse height to energy. Inset: FWHM as a function of fauxton frequency. (b) Histograms of single-shot device response to 24 THz fauxtons, 12 THz fauxtons, and no fauxtons. Response above T_c with no fauxtons is used to determine the contribution from amplifier noise.

determines the conversion from pulse height to fauxton frequency. The FWHM varies with the fauxton frequency, increasing from approximately 9 THz near saturation to 13 THz with no fauxtons (Fig. 4(a), inset). We speculate that this variation may be due to the pulse energy shifting the device toward a more optimum detection regime, similar to the

optimum pumping regime in superconducting bolometers operated as heterodyne mixers [9].

In Fig. 4(b) we show the histograms of 10^3 pulses for fauxton frequencies of 12 THz and 24 THz, as well as no fauxtons. We can distinguish between these different energies with nearly 90% fidelity. We also plot the histogram for no fauxtons with the device above T_c ($T = 0.35$ K) with the same bias voltage and probe power. Above T_c, the energy resolution should be limited by the amplifier noise. We find $\delta E_{amp} = 6.9$ THz FWHM. The intrinsic device noise and amplifier noise are assumed to be uncorrelated, and hence $\delta E_{total}^2 = \delta E_{amp}^2 + \delta E_{intrinsic}^2$.

We can calculate the intrinsic energy resolution due to thermal fluctuation and Johnson noise [6]. Using parameters appropriate for our device, we calculate $\delta E_{intrinsic,calc} = 6.3$ THz FWHM [5]. Adding this in quadrature to the measured amplifier noise, we predict $\delta E_{total,calc} = 9.3$ THz FWHM. This is consistent with the measured total energy resolution for higher fauxton frequencies.

Present devices have a spectral resolution $\lambda/\delta\lambda \approx 2.6$ at 24 THz. Future devices can achieve improved resolution by reducing the Ti nanobridge volume. For example, a device with reduced Ti dimensions of 0.5 μm x 0.1 μm x 50 nm and the same values of T_c, T_s and α has a calculated $\delta E_{intrinsic,calc} = 1.0$ THz [5].

We next consider the effect of amplifier noise on δE_{total} for this smaller volume device. We assume the device is voltage-biased. A change in resistance δR will result in a change in current δI given by $\delta I/I = \delta R/R$, where I and R are the steady state values of the device current and resistance, respectively. We define the current responsivity as the change in current δI divided by the absorbed energy δE. For a bolometric detector, the current responsivity is given by

$$\frac{dI}{dE} = \frac{\left(\frac{\delta R}{R} I\right)}{\left(C_e \, \delta T\right)} = \frac{I}{R}\left(\frac{dR}{dT}\right)\frac{1}{C_e}. \qquad (3)$$

The heat capacity C_e is proportional to the active device volume V. We assume R and dR/dT are independent of V. The Joule power I^2R from the bias current must heat the device to the same temperature (for a fixed T_c) and so should scale as V, and hence the bias current I should scale as $V^{1/2}$. Thus the responsivity dI/dE is proportional to $V^{-1/2}$.

The energy width due to amplifier current noise δI_{amp} is given by $\delta E_{amp} = \delta I_{amp}/(dI/dE)$. δI_{amp} is constant for a given device impedance (R_n is fixed at ≈ 50 Ω for efficient high frequency coupling). Hence δE_{amp} is proportional to $V^{1/2}$. From Equation (1) we see that $\delta E_{intrinsic}$ is also proportional to $V^{1/2}$. Thus the condition $\delta E_{amp} \approx \delta E_{intrinsic}$, which was demonstrated for the present device, will also hold for a smaller device with the same T_c using the same readout system. We conclude that amplifier noise will not prevent the realization of a significantly improved δE_{total} through the use of a smaller volume Ti device.

CONCLUSION

The fauxton characterization technique enables a straightforward experimental determination of the energy resolution of bolometric calorimeters. The performance of present devices achieves that predicted from measured device parameters, with an intrinsic energy resolution of approximately 6 THz FWHM. This can be reduced to approximately 1 THz FWHM by reducing the volume of the Ti nanobridge. Even further improvement is possible through the use of a device with a lower T_c.

ACKNOWLEDGMENTS

The work at Yale was supported in part by NSF-CHE-0616875 and Yale University. The work by B.K. and S.P. was carried out at the Jet Propulsion Laboratory, California Institute of Technology, under a contract with the National Aeronautics and Space Administration. The work at Rutgers was supported in part by NSF-ECS-0608842 and the Rutgers Academic Excellence Fund. B.R. acknowledges Yale support from the Flint Fund for Nanoscience for research visits during the summers of 2008 and 2009. L.F. acknowledges partial support from CNR-Istituto di Cibernetica, Pozzuoli, Italy.

REFERENCES

1. D. Leisawitz, *Adv. Space Res.* **34**, 631-636 (2004).
2. B. Swinyard and T. Nakagawa, *Exp. Astron.* **23**, 193-219 (2009).
3. B. S. Karasik and A. V. Sergeev, *IEEE Trans. Appl. Supercond.* **15**, 618-621 (2005).
4. P. R. Lawson *et al.*, *Proc. SPIE* **6268**, 626828 (2006).
5. D. F. Santavicca, B. Reulet, B. S. Karasik, S. V. Pereverzev, D. Olaya, M. E. Gershenson, L. Frunzio and D. E. Prober, submitted (2009); arXiv:0906.1205.
6. K. D. Irwin, Ph.D. dissertation, Stanford University (1995).
7. K. D. Irwin, *Appl. Phys. Lett.* **66**, 1998-2000 (1995).
8. J. Wei, D. Olaya, B. S. Karasik, S. V. Pereverzev, A. V. Sergeev and M. E. Gershenson, *Nature Nanotech.* **3**, 496-500 (2008).
9. P. J. Burke, R. J. Schoelkopf, D. E. Prober, A. Skalare, B. S. Karasik, M. C. Gaidis, W. R. McGrath, B. Bumble and H. G. LeDuc, *J. Appl. Phys.* **85**, 1644-1653 (1999).
10. P. L. Richards, *J. Appl. Phys.* **76**, 1-24 (1994).

Erratum

AIP Conf. Proc. **1185**, 72-75 (2009)

The experimental energy resolution reported here is smaller than was found in subsequent experiments. This is believed to be the result of a calibration error. For updated experimental results and analysis, please refer to *Appl. Phys. Lett.* **96**, 083505 (2010).